Establishing Direction during Chemotaxis in Eukaryotic Cells

Wouter-Jan Rappel,* Peter J. Thomas,† Herbert Levine,* and William F. Loomis‡

*Department of Physics, University of California, San Diego, La Jolla, California 92093-0319, †Computational Neurobiology Laboratory, Salk Institute for Biological Studies, San Diego, California 92186-5800, and ‡Division of Biology, University of California, San Diego, La Jolla, California 92093-0368 USA

ABSTRACT Several recent studies have demonstrated that eukaryotic cells, including amoeboid cells of *Dictyostelium discoideum* and neutrophils, respond to chemoattractants by translocation of PH-domain proteins to the cell membrane, where these proteins participate in the modulation of the cytoskeleton and relay of the signal. When the chemoattractant is released from a pipette, the localization is found predominantly on the proximal side of the cell. The recruitment of PH-domain proteins, particularly for Dictyostelium cells, occurs very rapidly (<2 s). Thus, the mechanism responsible for the first step in the directional sensing process of a cell must be able to establish an asymmetry on the same time scale. Here, we propose a simple mechanism in which a second messenger, generated by local activation of the membrane, diffuses through the interior of the cell, suppresses the activation of the back of the cell, and converts the temporal gradient into an initial cellular asymmetry. Numerical simulations show that such a mechanism is plausible. Available evidence suggests that the internal inhibitor may be cGMP, which accumulates within less than a second following treatment of cells with external cAMP.

INTRODUCTION

Chemotaxis, the ability of cells to respond to spatial and temporal gradients and determine the direction of their motion accordingly, is critical for many eukaryotic cell types (Devreotes, 1989). The amoeboid organism *Dictyostelium discoideum* has been widely recognized as a useful model system for the study of chemotaxis. In this system, developing cells use their chemotactic response to cAMP gradients to form aggregates. Genetic manipulations have revealed much of the architecture of the complex network underlying gradient sensing, and the workings of the network have been further elucidated by the use of subcellular fluorescence microscopy. Using this technique, it is now possible to investigate the intracellular dynamics of the components of the signaling network and to study how intracellular spatial and spatiotemporal patterns are involved in "deciding" which way the cell will move (Parent and Devreotes, 1999).

A recent set of papers has focused on the dynamics of PH (Pleckstrin Homology) domain proteins, including protein kinase B (PKB) and cytosolic regulator of adenylyl cyclase (CRAC) (Parent et al., 1998; Firtel and Meili, 2000). Upon stimulating a cell by the release of cAMP from a nearby pipette, a rapid (<2 s) recruitment of these proteins to the membrane closest to the pipette (which we will call the "front") was observed. Parts of the membrane further removed from the pipette (the "back") showed no such enhanced localization. This asymmetric recruitment presumably involves the PH domain binding to lipids modified by the action of PI3 kinases (Buczynski et al., 1997; van Es and Devreotes, 1999; Chung et al., 2001); a similar domain-specific interaction occurs in neutrophils (Servant et al., 2000).

These experiments demonstrate the establishment of an asymmetry within a few seconds after a rise of extracellular cAMP. This asymmetry is the first step in the directional sensing process of the cell. The surface membrane receptor for cAMP, CAR1, is uniformly distributed over the cell and cAMP will diffuse rapidly around the cell to the back. Also, the applied signal is several orders of magnitude larger than the value required to elicit a response. It is therefore necessary to presuppose an inhibitory mechanism that suppresses localization and other responses at the back. Thus, the basic sensing is done in a temporal manner, resolving the delay in excitation of the front versus the back. Once an initial asymmetry is established, it can be amplified and stabilized by mechanisms that respond to purely spatial differences in the chemoattractant concentration.

In this paper, we present a dynamical model that can account for this establishment of a rapid initial asymmetry via an inhibitory process mediated by the diffusion of an intracellular chemical messenger. As we will see, requiring the inhibitor to "win the race" against the activator places constraints on various kinetic rates; these constraints allow for the testing of our scheme. In particular, we propose a new dual stimulus experiment for which we present the model predictions. These predictions can be used to verify or disprove the assumed diffusive nature of inhibitor transport. We note that, should the diffusing-inhibitor approach be proven wrong, we would have to resort to more exotic mechanisms to explain the observations discussed above. The model does not attempt to describe the series of further responses that ultimately lead to pseudopod extension at the front and cortical rigor at the back, nor does it attempt to incorporate effects on a longer timescale including internal

Submitted February 18, 2002; and accepted for publication April 12, 2002.

Address reprint requests to Wouter-Jan Rappel, 9500 Gilman Dr., La Jolla, CA 92115. Tel: 858 822 1357; Fax: 858 534 7697; E-mail: rappel@physics.ucsd.edu.

0006-3495/02/09/1361/07 $2.00

cAMP production, establishment of polarity, and (de-)adaptation. However, it can account for the excitation and (de-)adaptation of cAMP-mediated cGMP production as observed in experiments (van Haastert and van der Heiden, 1983) (data not shown).

Our model is formulated in general terms and, at this level of abstractness, is independent of the exact nature of the second messenger. However, considering available experimental data, we have identified cGMP as the leading candidate to be the internal inhibitor. It is well known that cGMP accumulates rapidly upon activation and that small molecules diffuse freely through the cell interior (Wurster et al., 1977; van Haastert and van der Heiden, 1983; Segall, 1992; Potma et al., 2001). Moreover, mutants with impaired guanylyl cyclase activity show greatly reduced aggregation capability (Roelofs et al., 2001). This is consistent with our model, because response to cAMP traveling waves in vivo would use the same temporal mechanism to resolve the direction toward the aggregate center. Assuming that cGMP is our inhibitor, we discuss the specific predictions our model makes for several mutants.

THE MODEL

The binding of cAMP to the CAR1 receptor sets off a chain of events leading to the recruitment of PH domain proteins to a modified membrane (Parent and Devreotes, 1999; van Es and Devreotes, 1999; Meili et al., 2000). Because this process takes place in less than a second, it is essentially local along the membrane. We choose to ignore all the detailed steps involved in this process and instead introduce a three-state characterization of the membrane; quiescent (with density ρ_q), activated (with density ρ_a) and inhibited (with density ρ_i). The densities can take on values between 0 and 1 while the total density is conserved: $\rho_q + \rho_a + \rho_i \equiv 1$. The basic processes included in the dynamics of our model are: linear membrane activation due to the presence of extracellular cAMP ($q \rightarrow a$) at a rate α[cAMP]; linear membrane inhibition due to the presence of intracellular cGMP (q $\rightarrow$ i) at a rate β_r [cGMP]; and spontaneous transitions from activated to inhibited ($a \rightarrow$ i) at a rate δ and from inhibited to quiescent (i $\rightarrow$ q) at a rate β_f. The model is shown in Fig. 1. The activated state of the membrane is assumed to be responsible for the downstream events that lead to localization; we have not modeled this localization because there is little known quantitatively regarding its possible kinetics. The activated state of the membrane is also responsible for events on a longer time scale than several seconds, including the activation of adenylyl cyclase (after a delay of $\sim$1 min) and subsequent accumulation of cAMP within the cell and secretion of cAMP to relay the signal.

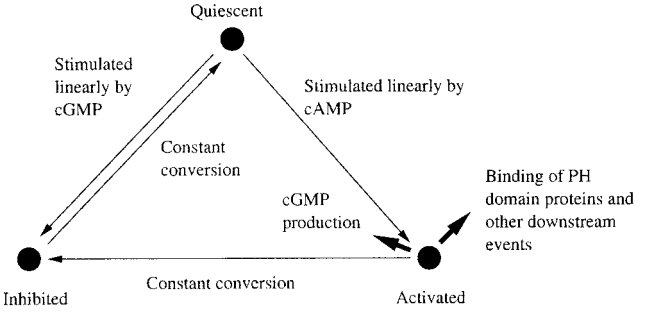

FIGURE 1 A schematic representation of our model. Before stimulation, the membrane is in the quiescent state. Upon stimulation with external cAMP, the membrane begins to enter the activated state, in which inter alia internal cGMP is produced. Internal cGMP puts quiescent membrane into the inhibited state, pre-empting activation in the back of the cell where the external cAMP arrives more slowly. The activated state also leads to downstream events, including localization of PH domain binding proteins to the membrane and eventually pseudopod extension.

The equations governing the membrane state are

$$\frac{\partial \rho_q}{\partial t} = -\alpha c \rho_q + \beta_f \rho_i - \beta_r g \rho_q,$$

$$\frac{\partial \rho_a}{\partial t} = \alpha c \rho_q - \delta \rho_a, \qquad (1)$$

$$\frac{\partial \rho_i}{\partial t} = -\beta_f \rho_i + \beta_r g \rho_q + \delta \rho_a,$$

which conserve the total receptor density. We have taken the activation and inhibition to be first order in the concentrations at the membrane of extracellular cAMP (c) and intracellular cGMP (g), respectively. In the bulk, these concentrations obey the diffusion equations

$$\frac{\partial c}{\partial t} = D_c \vec{\nabla}^2 c - \mu_c c \qquad \frac{\partial g}{\partial t} = D_g \vec{\nabla}^2 g - \mu_g g, \qquad (2)$$

in the extracellular and intracellular spaces, respectively. The decay term μ_c represents extracellular cAMP-specific phosphodiesterase activity (taken to be zero for the time scale considered in this paper), and μ_g represents intracellular cGMP-specific phosphodiesterase activity. The bulk equations are solved via a finite-element method on an irregular lattice where the intersection of the interior and exterior nodes forms the set of membrane nodes. We generate the grid using standard methods (MATLAB's PDE Toolbox, The Mathworks, Natick, MA) and the interaction matrices used to solve the diffusion equation with zero-flux boundary conditions separately for each reactant,

$$D_g \hat{n} \cdot \vec{\nabla} g = D_c \hat{n} \cdot \vec{\nabla} c = 0, \qquad (3)$$

where $\hat{n}$ is the normal of the membrane. At the nodes corresponding to the boundary, the cGMP field has an

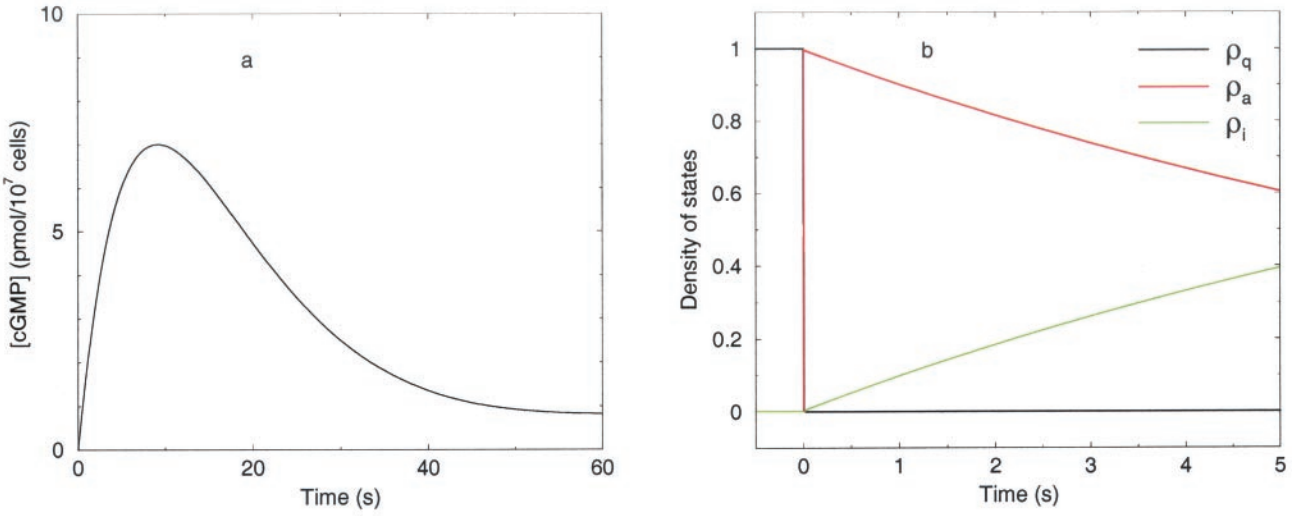

FIGURE 2 (*a*) The total cGMP after uniform addition of cAMP. (*b*) The corresponding density of membrane states for the first 5 s. The density of quiescent state (ρ_q, *black line*), drops rapidly from 1 to nearly zero as the cAMP stimulus is presented. The density of activated state (ρ_a, *red line*) rises sharply and is subsequently slowly converted into the inhibited state (ρ_i, *green line*).

additional source term that accounts for the production of cGMP by the membrane,

$$\frac{\partial g_{\text{boundary}}}{\partial t} = \sigma_g \rho_a + \text{bulk terms}. \quad (4)$$

The finite-element scheme generates a set of nonlinear ordinary differential equations (ODEs) for the evolution of the concentrations at each node. We solve the ODEs with a variable time-step fourth-order Runge–Kutta method (using built-in ODE solvers in MATLAB v5.2, which approximates the finite-element mass matrix by the identity matrix).

For simplicity, we treated cells as two-dimensional disks. We have checked that generalizing to ellipsoids makes no important difference in the results. The cell is placed in a square domain, representing the bath. The model cell was chosen to have a diameter of 10 μm and the bath was 30 $\times$ 30 μm. The diffusion constant of external cAMP and internal cGMP was taken to be identical: $D_c = D_g = 2.5 \times 10^{-6}$ cm^2/s. To relate the remaining parameters of our two-dimensional model to volume quantities, we assume that the cell has a height of 1 μm. Furthermore, we equated the peak of the total [cGMP] produced after a uniform stimulus of cAMP (see below) to the experimentally observed value of 7 pmol/10^7 cells.

RESULTS

Uniform cAMP stimulus

To demonstrate the dynamics of our model and to fix several of our model parameters, we first subjected the cell to a uniform increase of external cAMP. Here, and elsewhere in this paper, we choose as the initial condition the steady-state solution of Eqs. 1–3 in the absence of a stimulus, i.e., $\rho_a = \rho_i = g = c = 0$ and $\rho_q = 1$. This steady state should be interpreted as the state in which the membrane has adapted itself and no longer responds to any possible background levels of external cAMP. A stimulus represents an increase of cAMP above the background level.

The stimulus is modeled by simply setting c well above threshold throughout the extracellular domain at t = 0 (assumed to correspond to a pipette concentration of 1 μM). The total cGMP in the cell is plotted as a function of time in Fig. 2 *a*. We have adjusted the parameter values such that the peak time of total cGMP production is consistent with experimentally observed values and occurs at roughly 10 s. Furthermore, also based on experimental results, we have chosen the parameter values such that, after 30 s, the total cGMP has been reduced to 30% of its peak value. In practice, the adjustment was achieved as follows. After finding a range of parameters that resulted in a significant asymmetric response to an asymmetric cAMP stimulus (see below) we chose the production rate (σ^g) and phosphodiesterase rate (μ_g) of cGMP that resulted in a correct time course of the total cGMP. The final parameter values can be found in Table 1.

The dynamics of the membrane states after delivering cAMP is plotted in Fig. 2 b. Before the addition of cAMP, all of the membrane is in the quiescent state (*black line*). Directly after sensing the increase in c, there is a rapid conversion to the activated state (*red line*). The activated state produces a fast increase in cGMP which, in turn, converts the remainder of the quiescent state directly into the inhibited state (*green line*). The depletion of the quiescent state takes place in less than 0.01 s. The inhibited state

TABLE 1 Parameter values used throughout this paper

$D_c = D_g$	2.5×10^{-6} cm^{2}s^{-1}
α	2400 $(\mu$Ms$)^{-1}$
β_f	0.01 s^{-1}
β_r	0.22 $(\mu$Ms$)^{-1}$
δ	0.1 s^{-1}
μ_c	0.0 s^{-1}
μ_g	0.12 s^{-1}
σ_g	0.14 M/s

D_c and D_g, diffusion constants of cAMP and the intracellular inhibitor, respectively; α, rate of membrane activation in response to extracellular cAMP; β_f, rate of return to the quiescent state from the inhibited state; β_r, rate of membrane inhibition in response to the intracellular inhibitor; δ, transition rate from the activated state to the inhibited state; μ_c and μ_g, decay rates of cAMP and the inhibitor, respectively; σ_g, production rate of the inhibitor by the activated membrane state. The total receptor density is constant and taken to be 1.

then slowly converts back to the quiescent state as cGMP is removed by the cGMP-specific phosphodiesterase activity. Similar results were obtained when the cAMP stimulus was limited to several seconds (data not shown).

Asymmetric cAMP stimulus

Next, we introduced an asymmetric cAMP stimulus in our computational domain. To this end, we clamp the value of cAMP to a value well above threshold at the upper left corner of our grid at the onset of the simulation. Of course, the precise location of our source can be changed and does not affect the qualitative outcome of the numerical experiment. Figure 3 a shows the time course of various quantities at the front of the cell (*solid lines*) and at the back of the cell (*dashed lines*). Plotted are the cAMP concentration (*black lines*), the cGMP concentration (*red lines*) and the density of the activated state (*green lines*). Figure 3 b shows the same graph between time −0.25 and 2 s. As illustrated in the figures, the cAMP concentration increases first at the front of the cell. Consequently, the membrane, which was in its quiescent state, is activated and starts to produce cGMP. This cGMP diffuses through the cell while the cAMP diffuses around the cell. The local concentration of cGMP increases dramatically at the leading edge, allowing cGMP levels to rise quickly enough at the back of the cell to inhibit the activation of the membrane. Thus, the fast-diffusing second inhibitory messenger has created an asymmetry in the density of the activated state in the cell. This asymmetry can be characterized by the asymmetry ratio (AR), defined as the ratio of the peak values of the density of the activated state at the front and at the back. For the parameter values of Table 1, this ratio is 4.9.

The upper row in Fig. 4 shows the density of the activated state along the membrane of the cell at increasing times as a gray-scale plot with white corresponding to a high density and black corresponding to a low density of the activated state. We see that the density of the activated state decreases continuously between the front of the cell (marked with F) and the back of the cell (marked with B). Because the translocalization of the PH domain proteins is driven by the activated state of the membrane, the patterns observed for GFP-tagged PH domain proteins should be qualitatively identical. However, it should be pointed out that this translocation, and other downstream processes, can involve a threshold event. Thus, the resulting distribution of PH domain proteins need not be a continuous function of the position along the cell membrane.

It is clear that our model requires either a large enough production rate of the inhibitor or a fast enough transition

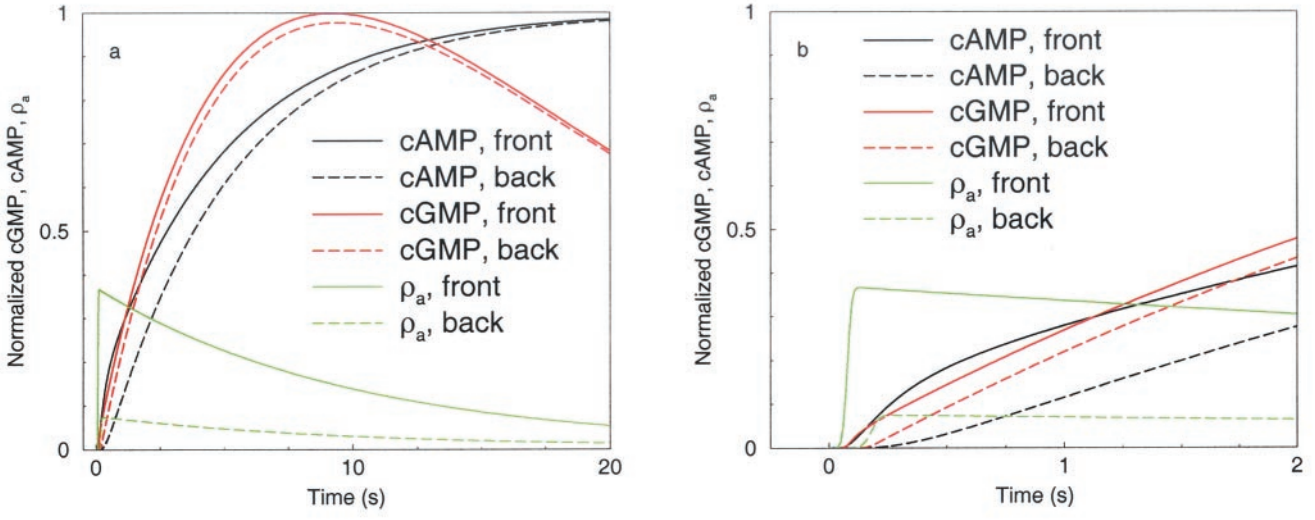

FIGURE 3 (*a*) cAMP, cGMP, and density of activated state as a function of time for the front and the back of the cell. The cAMP and cGMP curves are normalized by their peak values at the front of the cell. (*b*) Blow-up of the same graph displaying the first two seconds.

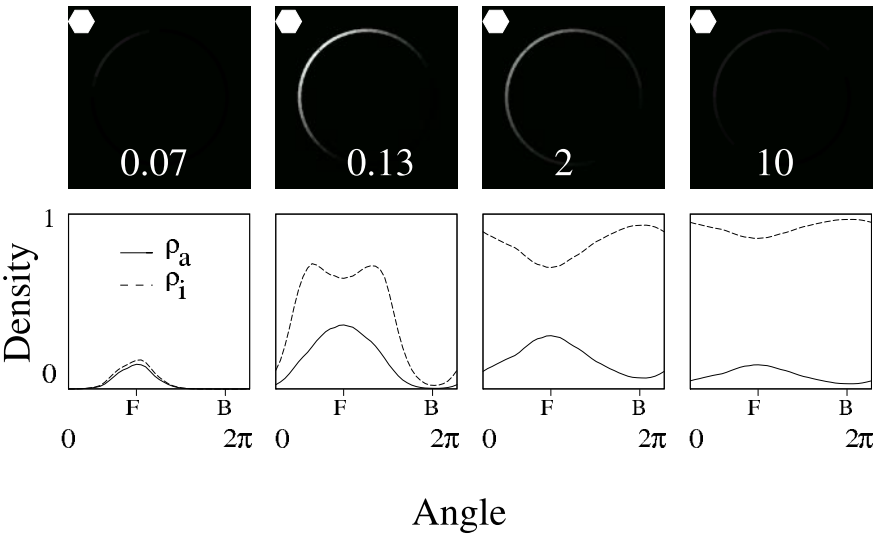

FIGURE 4 *Upper row*, gray-scale plots of the activated state along the membrane of the cell for different times (measured in seconds). White corresponds to a high density and black corresponds to a low density. The hexagon represents the source of cAMP, which is located in the upper left corner. The density of the activated state (*solid line*) and of the inhibited state (*dashed line*) is plotted for the same times in the graphs on the lower row. The membrane position is plotted in polar coordinates with the front of the cell marked by F and the back of the cell marked by B. The activated state attracts PH domain proteins to the membrane resulting in membrane localization patterns that are similar to the ones displayed in the upper row.

from the quiescent state to the inhibited state. In fact, because the transformations $\sigma_g \rightarrow \lambda\sigma_g$ and $\beta_r \rightarrow \beta_r/\lambda$ is equivalent to a simple rescaling of g in Eqs. 1 and 4 the AR remains constant for fixed values of the product $\sigma_g\beta_r$. Similar, less obvious relationships can also be found. For example, for the parameter values in Table 1, we found that the AR remains roughly fixed for a fixed ratio of α/β_r, indicating that increasing the rate from quiescent to activated will decrease the AR unless the transition rate from quiescent to inhibited is also increased.

Sensitivity to model parameters

To check the sensitivity to model parameter values and the robustness of our model we have varied parameter values in our model in a systematic way. Starting with the parameter values for α, β_f, β_r, δ, and σ_g of Table 1, we have multiplied and divided these parameters by either 2 or 5. Allowing all possible combinations, we measured $5^3 = 243$ ARs. Histograms were produced by normalizing the AR by the AR corresponding to the baseline parameter set (AR = 4.9) and binning the data into bins with width 0.1. The results are shown in Fig. 5. As expected, allowing the parameters to change fivefold leads to an increased spread in ARs. The important point, however, is that Fig. 5 shows that our model is not very sensitive to parameter values. For example, for the twofold variation, roughly half of the ARs are within 10% of the baseline AR. In addition, as can be clearly seen in Fig. 5, the AR of our baseline set of parameters is by no means the optimal AR of our model. Thus, significant ARs can be achieved for a wide range of parameters.

Dual cAMP stimulus

To further elucidate the critical timing issues in our model, we devised a novel experiment. In this experiment, we deliver cAMP in one corner of the grid as described above,

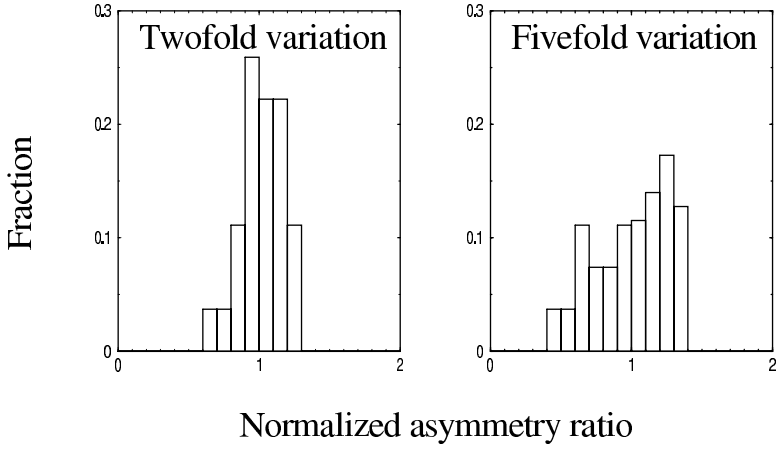

FIGURE 5 Histograms for the asymmetry ratio, normalized by the asymmetry ratio corresponding to baseline set of parameter values of Table 1, for twofold and fivefold variation of parameters α, β_f, β_r, δ, and σ_g.

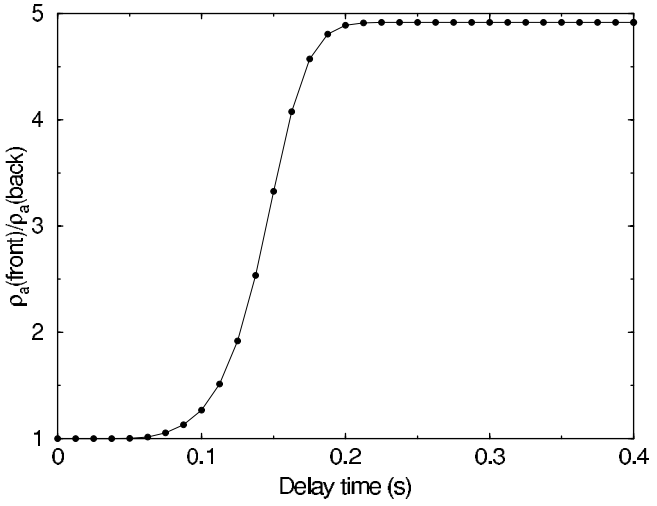

FIGURE 6 Density of activated states at the front normalized by the density of activated states at the back as a function of delay time. The cell is stimulated first at the front followed, after a time delay, by a stimulus at the back.

followed, after a time delay, by delivery of cAMP at the opposite corner of the grid. We have performed such an experiment using our numerical model, and our results are shown in Fig. 6, where we plot the AR as a function of the time delay. As expected, for very small time delays, the cGMP production at the front and the back are nearly identical and the AR approaches 1. As the time delay is increased, the AR rises continuously until it reaches the value for the single stimulus experiment (AR = 4.9). Experiments should show a similar sigmoidal response in PH domain protein translocalization as in Fig. 6.

DISCUSSION

We have presented a model that can account for fast inhibition of the *Dictyostelium* cell membrane in the presence of an activation wave of cAMP. The essential ingredient of our model is a rapidly diffusing inhibitory second messenger. In our model, this second messenger can act so that a significant portion of the membrane at the back of the cell will go into its inhibited state before it can be activated by the external cAMP. This leads to an asymmetry between the back and the front of the cell that is established in less than one second and which is the first step in the cell's process to determine its direction. Recall that, during the aggregation stage, cells encounter cAMP waves roughly every 6 min. The need for the cell to establish a signal-based asymmetry has been recognized (Ueda et al., 2001), at least up to the point when they become significantly polarized. Our model presents a possible mechanism for this. Every 6 min a cell, after having returned to its quiescent state, is presented with a rise in external cAMP. Through the temporal mechanism presented here, the cell uses this spatio-temporal signal to establish the needed directional information.

It is important to realize that, in our model, the concentration of cGMP at the back of the cell need not be large compared to the concentration of external cAMP. Small concentrations can still inhibit the membrane, provided that the rate from quiescent state to the inhibited state (β_r) is large enough. This also means that the same mechanism can still work if some of the parameter values and constraints are relaxed. For example, using an ellipsoid with large eccentricity will reduce the diffusional path difference between the external cAMP and the internal cGMP. However, by increasing the sensitivity of the membrane to cGMP and/or production rate, we can still produce a significant AR. A possible reduction of the diffusion constant of cGMP can be compensated in a similar fashion.

A direct verification of the mechanisms presented here can be obtained from the proposed dual stimulus experiment. The behavior of localization to the membrane should be radically altered when increasing the time delay between the two deliveries (see Fig. 6). For small time delays, the localization should be uniform. Upon increasing the time delay, the localization should appear more and more asymmetrical. Note that this experiment offers a test for the model that does not require the identification of the second messenger.

We have argued here that a likely candidate for the inhibitor is cGMP, which is known to accumulate rapidly in the cell upon sensing a rise in external cAMP. On the basis of the assumption that cGMP is our inhibitor, we can make predictions regarding the localization of PH domain proteins in mutants with reduced cGMP production. These mutants should not exhibit the front–back asymmetry shown in Fig. 3. Thus, in guanylyl cyclase mutants, PH domain proteins such as CRAC should translocate more uniformly to the cell membrane than they would in the wild-type upon stimulation from one side.

Our model, by construction, focuses on the first few seconds of the response. We expect that the initial asymmetry caused by the timing difference between the front and the back will be amplified or stabilized by the (almost static) cAMP gradient that follows. This is consistent with experimental results that show that cells in long-lasting gradients develop a well-established polarity and eventually, no longer need the temporal "priming." Overall, our temporal-first scheme is rather different than the static gradient sensing models proposed by several other research groups (Meinhardt, 1999; Narang et al., 2001; Postma et al., 2001). In fact, our model suggests that directed motion would not occur in physiologically reasonable, purely static gradients. Experimental attempts to clarify this picture are difficult because creating a static gradient without first encountering a temporal signal is problematic. Several such attempts have been undertaken with results that have been interpreted as consistent with this prediction (Vicker et al., 1984; Vicker,

1994). However, carefully controlled experiments on single cells, combined with subcellular microscopy techniques, have not been carried out yet. These experiments should be helpful in aiding our understanding of chemotaxis.

W.I.R., H.L. and W.F.L. acknowledge support from the National Science Foundation Biocomplexity program. P.J.T. was supported by the Sloan–Swartz Center for Theoretical Neurobiology at the Salk Institute for Biological Studies.

REFERENCES

Buczynski, G., B. Grove, A. Nomura, M. Kleve, J. Bush, R. A. Firtel, and J. Cardelli. 1997. Inactivation of two *Dictyostelium discoideum* genes, DdPIK1 and DdPIK2, encoding proteins related to mammalian phosphatidylinositide 3-kinases, results in defects in endocytosis, lysosome to postlysosome transport, and actin cytoskeleton organization. *J. Cell Biol.* 136:1271–1286.

Chung, C. Y., G. Potikyan, and R. A. Firtel. 2001. Control of cell polarity and chemotaxis by Akt/PKB and PI3 kinase through the regulation of PAKa. *Mol. Cell.* 7:937–947.

Devreotes, P. N. 1989. *Dictyostelium discoideum:* a model system for cell–cell interactions in devel-opment. *Science.* 245:1054–1058.

Firtel, R. A., and R. Meili. 2000. *Dictyostelium:* a model for regulated cell movement during mor-phogenesis. *Curr. Opin. Genet. Devel.* 10: 421–427.

Meili, R., C. Ellsworth, and R. A. Firtel. 2000. A novel Akt/PKB-related kinase is essential for morphogenesis in *Dictyostelium. Curr. Biol.* 10:708–717.

Meinhardt, H. 1999. Orientation of chemotactic cells and growth cones: models and mechanisms. *J. Cell. Sci.* 112:2867–2874.

Narang, A., K. K. Subramanian, and D. A. Lauffenburger. 2001. A mathematical model for chemoattractant gradient sensing based on receptor-regulated membrane phospholipid signaling dynamics. *Ann. Biomed. Eng.* 29:677–691.

Parent, C. A., B. J. Blacklock, W. M. Foehlich, D. B. Murphy, and P. N. Devreotes. 1998. G protein signaling events are activated at the leading edge of chemotactic cells. *Cell.* 95:81–91.

Parent, C. A., and P. N. Devreotes. 1999. A cell's sense of direction. *Science.* 284:765–770.

Postma, M. and P. J. M. Van Haastert. 2001. A diffusion-translocation model for gradient sensing by chemotactic cells. *Biophys. J.* 81: 1314–1323.

Potma, E. O., W. P. De Boeij, P. J. M. Van Haastert, and D. A. Wiersma. 2001. Real-time visual-ization of intracellular hydrodynamics in single living cells. *Proc. Natl. Acad. Sci., U.S.A.* 98: 1577–1582.

Roelofs, J., J. Meima, P. Schaap, and P. J. M. Van Haastert. 2001. The *Dictyostclium* homologue of mammalian soluble adenylyl cyclase encodes a guanylyl cyclase. *EMBO J.* 20:4341–4348.

Segall, J. E. 1992. Behavioral responses of streamer F mutants of *Dictyostelium discoideum:* effects of cyclic GMP on cell motility. *J. Cell. Sci.* 101:589–597.

Servant, G., O. D. Weiner, P. Herzmark, T. Balla, J. W. Sedat, and H. R. Bourne. 2000. Polarization of chemoattractant receptor signaling during neutrophil chemotaxis. *Science.* 287:1037–1040.

Ueda, M., Y. Sako, T. Tanaka, P. N. Devreotes, and T. Yanagida. 2001. Single-molecule analysis of chemotactic singaling in *Dictyostelium* cells. *Science.* 294:864–867.

Van Es, S., and P. N. Devreotes. 1999. Molecular basis of localized responses during chemotaxis in amoebae and leukocytes. *Cell. Mol. Life Sci.* 55:1341–1351.

Van Haastert, P. J. M., and P. R. Van Der Heijden. 1983. Excitation, adaptation, and deadaptation of the cAMP-mediated cGMP response in *Dictyostelium discoideum. J. Cell. Biol.* 96:347–353.

Vicker, M. G., W. Schill, and K. Drescher. 1984. Chemoattraction and chemotaxis in *Dictyostelium discoideum:* myxamoeba cannot read spatial gradients of cyclic adenosine monophosphate. *J. Cell. Biol.* 98: 2204–2214.

Vicker, M. G. 1994. The regulation of chemotaxis and chemokinesis in *Dictyostelium* amoebae by temporal signals and spatial gradients of cyclic AMP. *J. Cell. Sci.* 107:659–667.

Wurster, B., K. Schubiger, V. Wick, and G. Gerish. 1977. Cyclic GMP in *Dictyostelium discoideum,* oscillations and pulses in response to folic acid and cyclic AMP signals. *FEBS Lett.* 76:141–144.